④

AFGL-TR-88-0057

SSS-R-88-9339
W/O 11304

Charging Potentials for Two Sample Sets of Spectra from DMSP Satellites

T. G. Barker

S-CUBED
A Division of Maxwell Laboratories, Inc.
P. O. Box 1620
La Jolla, CA   92038

February 1988

Scientific Report No. 8

AIR FORCE GEOPHYSICS LABORATORY
AIR FORCE SYSTEMS COMMAND
UNITED STATES AIR FORCE
HANSCOM AIR FORCE BASE
MASSACHUSETTS   01731

DTIC
ELECTE
10 JAN 198?
E

AD-A203 694
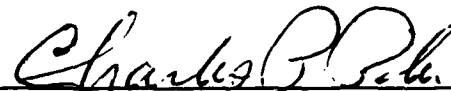
89   1 09 237

" This technical report has been reviewed and is approved for publication "
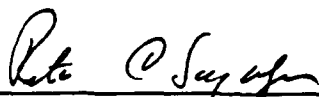

DAVID L. COOKE
Contract Manager

CHARLES P. PIKE
Branch Chief

FOR THE COMMANDER

RITA C. SAGALYN
Division Director

This report has been reviewed by the ESD Public Affairs Office (PA) and is releasable to the National Technical Information Service (NTIS).

Qualified requestors may obtain additional copies from the Defense Technical Information Center. All others should apply to the National Technical Information Services.

If your address has changed, or if you wish to be removed from the mailing list, or if the addressee is no longer employed by your organization, please notify AFGL/DAA, Hanscom AFB, MA 01731. This will assist us in maintaining a current mailing list.

Do not return copies of this report unless contractual obligations or notices on a specific document requires that it be returned.

ADA203694

REPORT DOCUMENTATION PAGE

1a. REPORT SECURITY CLASSIFICATION Unclassified			1b. RESTRICTIVE MARKINGS
2a. SECURITY CLASSIFICATION AUTHORITY N/A			3 DISTRIBUTION / AVAILABILITY OF REPORT Approved for public release: distribution unlimited
2b. DECLASSIFICATION / DOWNGRADING SCHEDULE N/A			
4 PERFORMING ORGANIZATION REPORT NUMBER(S) SSS-R-88-9339			5. MONITORING ORGANIZATION REPORT NUMBER(S) AFGL-TR-88-0057
6a. NAME OF PERFORMING ORGANIZATION S-CUBED, A Division of Maxwell		6b. OFFICE SYMBOL (If applicable)	7a. NAME OF MONITORING ORGANIZATION Air Force Geophysics Laboratory
6c. ADDRESS (City, State, and ZIP Code) P. O. 1620 La Jolla, CA 92038-1620			7b. ADDRESS (City, State, and ZIP Code) Hanscom Air Force Base, MA. 01731-5320
8a. NAME OF FUNDING / SPONSORING ORGANIZATION Air Force Geophysics Laboratory		8b OFFICE SYMBOL (If applicable)	9 PROCUREMENT INSTRUMENT IDENTIFICATION NUMBER F19268-86-C-0056

8c. ADDRESS (City, State, and ZIP Code) Hanscom Air Force Base, MA 01731-5320	10 SOURCE OF FUNDING NUMBERS			
	PROGRAM ELEMENT NO	PROJECT NO	TASK NO	WORK UNIT ACCESSION N
	62101F	7601	30	AA

| 11 TITLE (Include Security Classification) Charging Potentials for Two Sample Sets of Spectra from DMSP Satellites |

| 12. PERSONAL AUTHOR(S) T. G. Barker |

13a. TYPE OF REPORT Interim technical report No. 8	13b. TIME COVERED FROM 1/88 TO 2/88	14 DATE OF REPORT (Year, Month, Day) February, 1988	15 PAGE COUNT 18

| 16. SUPPLEMENTARY NOTATION |

17 COSATI CODES			18 SUBJECT TERMS (Continue on reverse if necessary and identify by block number)
FIELD	GROUP	SUB-GROUP	Spacecraft charging; DMSP satellite, POLAR, POLAR auroral charging

19. ABSTRACT (Continue on reverse if necessary and identify by block number)

Katz, Mandell, Jongeward, and Gussenhoven [1986] discuss the importance of accurately including the emission of secondary and backscattered electrons in the calculations of flux balances that are used to predict the equilibrium potential of satellites during intense electron precipitation. We have applied this concept to a sequence of electron and ion flux spectra observed by DMSP satellites to determine the levels of negative charging, if any, experienced by the satellites. The net electron current [incident minus backscattered and secondary electrons is a diagnostic quantity that can be used to determine whether charging has occurred. Using simple models of the satellite and ion collection, along with secondary and backscatter yields for the appropriate covering, one can quickly scan large amounts of data for charging events and estimate the equilibrium potential.

20. DISTRIBUTION / AVAILABILITY OF ABSTRACT ☐ UNCLASSIFIED/UNLIMITED ☐ SAME AS RPT. ☐ DTIC USERS	21. ABSTRACT SECURITY CLASSIFICATION Unclassified
22a. NAME OF RESPONSIBLE INDIVIDUAL Dr. David L. Cooke	22b. TELEPHONE (Include Area Code) 22c. OFFICE SYMBOL AFGL/PHK

DD FORM 1473, 84 MAR   83 APR edition may be used until exhausted.   SECURITY CLASSIFICATION OF THIS PAGE
All other editions are obsolete.

TABLE OF CONTENTS

CHARGING POTENTIALS FOR TWO SAMPLE SETS
OF SPECTRA FROM DMSP SATELLITES

T. G. Barker

S-CUBED Division of Maxwell Laboratories, Inc.

1. INTRODUCTION

Katz, Mandell, Jongeward, and Gussenhoven (1986) discuss the importance of accurately including the emission of secondary and backscattered electrons in the calculations of flux balances that are used to predict the equilibrium potential of satellites during intense electron precipitation. We have applied this concept to a sequence of electron and ion flux spectra observed by DMSP satellites to determine the levels of negative charging, if any, experienced by the satellites. The net electron current (incident minus backscattered and secondary electrons) is a diagnostic quantity that can be used to determine whether charging has occurred. Using simple models of the satellite and ion collection, along with secondary and backscatter yields for the appropriate covering, one can quickly scan large amounts of data for charging events and estimate the equilibrium potential.

2. METHODS OF ANALYSIS

Our approach is to compute the incident and net fluxes from the observed spectra, assume an ion collection model, and then compute the potential. The observations are treated as discretizations of a continuous flux, which are then numerically integrated with respect to energy to find the total and net fluxes. The details of the method and possible sources of error are discussed in Barker (1986). The method described here is meant to be a tool for analyzing large quantities of data so the techniques are simple and computationally fast. The calculations do not involve the nonlinear, iterative schemes to solve for charging voltage that are used in other S-CUBED charging programs but employ simple methods that perhaps sacrifice some accuracy for speed. In the following, we describe these methods.

2.1 Calculations of Currents

The electrons incident on a satellite generate secondary and backscattered currents. The net current for electrons impinging uniformly from all directions is found using Lai, Gussenhoven, and Cohen (1983); Olsen (1983); and Katz, Parks, Mandell, Harvey, Brownell, Wang, and Rotenberg (1977):

$$J_{net}^{electron} = \pi e_{el} \int_0^\infty [1 - Y(E) - B(E)] \Phi_{el}(E) dE$$

(2.1)

Here, $Y(E)$ and $B(E)$ are the secondary and backscattered yields, $\Phi_{el}(E)$ is the observed electron spectrum, and e_{el} is the charge of an electron. The functions are determined numerically by the S-CUBED computer program, MATCHG. The code, MATerial CHarGing, uses the sophisticated models of secondary electron emission and backscatter developed for the NASCAP code (Katz [1978] and Katz [1986]) and employed in the POLAR code (Lilley et al. [1985]). The integrals for net current are performed numerically using tables of Y and B.

In principle, the ion current could be found in a similar fashion. For ions, backscattered yields are negligible, and

$$J_{net}^{ion} = -\pi e_{el} \int_0^\infty [1 + Y_{ion}] \Phi_{ion}(E) dE$$

(2.2)

gives the ion current for the observed spectrum $\Phi_{ion}(E)$. The sign of the secondary yield is positive because electrons are emitted rather than ions. It should also be possible to infer the ambient ion density and temperature from $\Phi_{ion}(E)$ and experimental values of Y_{ion}. Secondary yields for metallic substances have recently become available (Langley et al. [1984]) but not for materials such as teflon and kapton. In addition, the energy of ambient ions are below the energy band of the DMSP collectors (1 eV to 30 keV) and are not detected, so that $\Phi_{ion}(E)$ is incompletely determined.

2.2 Calculations of Yield Curves

The secondary and backscatter electron yields are dependent on the angular distribution of the incident flux and the covering material (type and distribution on the surface). Since the yield curves are not strongly affected by the distribution of angles of incidence, and since there are no observations of incidence angles, we have

assumed isotropy. The total flux estimated from the measured spectrum also depends on the angular distribution of incident electrons. This affects the estimate through an areal scale factor. We point out that if information becomes available indicating anisotropy is important, then these effects could be readily included, especially since MATCHG already computes yield curves for beamed electrons.

The covering material determines the proportions of secondary and backscattered electrons. The "charge" program incorporates this by reading files written by MATCHG listing yields as functions of energy for each material of interest. These files are described in the manual, which constitutes the appendix of Barker (1986). Details of the calculation of yield curves are given in Katz et al. (1977). In the interest of computational speed, a uniform surface covering is assumed and a 1-D charge calculation is done. If the satellite has concave surfaces or coverings with strong variations in backscattering properties, then a 3-D approach is warranted. The success of Katz et al. (1986) in matching calculated charging voltages with DMSP observations using a 1-D approach indicates that the assumption of uniform covering is probably justified.

2.3 Ion Collection Mechanism and Potential Calculations

Katz et al. (1986) showed that for the DMSP satellite, ion collection is orbit-limited; so we have used this model for our study. Again, in the interest of computational speed, we have made an approximation to the charging calculation by using only one iteration for voltage. That is, the charging voltage V satisfies

$$J^{ion} + J^{electron}_{net} = 0 \qquad (2.3)$$

where

$$J^{electron}_{net} = \pi e_{el} \int_V^{\infty} (1 - Y - B)(1 - \frac{V}{E}) \phi(E)\,dE \qquad (2.4)$$

and the ion current is computed using the orbit-limited mechanism. To find the voltage V, one computes the net electron current with an initial lower limit E = 0, then finds the voltage that gives an ion current satisfying (2.3). This voltage is then used to compute the lower limit for (2.4), and the processed is repeated until

convergence. For this study, we have performed only the first iteration. This is valid as long as the charging voltages are small compared to the electron energies.

3. OBSERVATIONS

The Air Force Geophysics Laboratory has supplied two data sets that are sequences of electron and ion differential flux spectra from two DMSP satellites, F6 and F7. The observations span different time periods, 44,100 to 44,160 and 1,740 to 1,836, and are spaced at 2-second intervals. The DMSP collectors and their calibrations are described in Hardy et al. (1984). The detectors sample the flux spectrum at 20 energies whose logarithms are spaced at equal intervals between 1 eV and 30 keV. The spectral values in the data files provided to us were in the form of differential fluxes, having been converted from digital counts using the geometrical factors described by Hardy et al. (1984).

Numerous flux values in the data set are identically zero. We note that flux values at energies adjacent to the ones that are zero are well above the least count level, indicating that the zeroes are not due to lack of resolution in digitization. We have assumed that zero data are the result of problems in recording or transmission. For the purposes of our analyses, we have replaced zero values by interpolating between nonzero values.

4. RESULTS OF ANALYSES

The objectives of this study are to develop a computational tool which can scan a large number of spectra for events that charge and to predict the charging level. To satisfy the first task, we require a feature of the data that is diagnostic of charging, and which can be extracted from the data using an automatic procedure that requires no intervention by the analyst.

DeForest (1972) has shown that charging events have increased flux levels at high energies and a cutoff energy ($= e_{el}V$) below which there is no ion flux, indicating that ions are being accelerated towards the detector as a result of the charging and that only ions generated within the sheath would enter the detector with energy less than the cutoff. We propose here another method that uses the net electron current, as computed by Equation (2.1). This method is simple and readily automated.

Consider the orbit limited ion collection model for which the potential satisifies

$$V = T_S \left[\frac{J^{electron}_{net}}{J^{ion}_{net}} + 1 \right]$$

$$\tag{4.1}$$

where for typical low earth and polar orbits, T_S = 5 Volts and

$$J^{ion}_{net} = \frac{1}{4} n_{ion} e \mid v_{sat}$$

$$\tag{4.2}$$

Here, n_{ion} is the ion density and v_{sat} is the satellite velocity ($\sim$ 8 km/sec). The charging condition of interest is when V in (4.1) is negative. Since J^{ion}_{net} is positive (backscatter and secondaries for ions are negligible), this requires that $J^{electron}_{net}$ be negative and greater than J^{ion}_{net} in absolute value. An initial screening of the data can be achieved without knowledge of J^{ion}_{net} by looking for negative values of $J^{electron}_{net}$.

As can be seen in (2.1), $J^{electron}_{net}$ depends not only on the electron flux spectrum but on its product with 1 - Y(E) - B(E), the net differential flux at energy E integrated over the energy band. Fig. 4.1 shows the functions Y(E), B(E), and 1 - Y - B for teflon and kapton, respectively. The main body of the satellite has surfaces which are primarily teflon or kapton. The function 1 - Y - B decreases sharply from zero
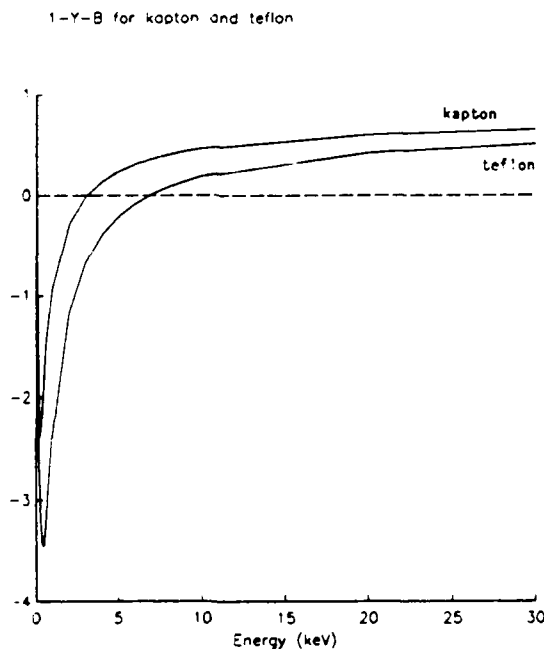

Fig. 4.1   The function 1 - Y(E) - B(E), the relative electron flux weighting function, is shown for two covering materials, teflon and kapton.

to a peak negative value at a low energy, then increases through zero and levels out at high energies. The most important difference between the curves for the two materials for the purposes of this study is the energy at which the function crosses zero: about 3 keV for kapton and 12 keV for teflon. In order that $J_{net}^{electron}$ be negative, or equivalently, that the integral

$$I = \int_0^\infty [1 - Y(E) - B(E)]\phi_{el}(e)dE$$

(4.3)

be positive ($e_{el} < 0$), the spectrum must be small at low energies (where 1 - Y - B < 0) and large at high energies. Thus, the inverted V spectrum is often associated with charging conditions.

We have computed $J_{net}^{electron}$ for the two data sets of the surface covering materials teflon and kapton. Fig. 4.2 and 4.3 show $J_{net}^{electron}$ for the time period 1,740 to 1,836; and Fig. 4.4 and 4.5 show it for 44,100 to 44,160. For both surface
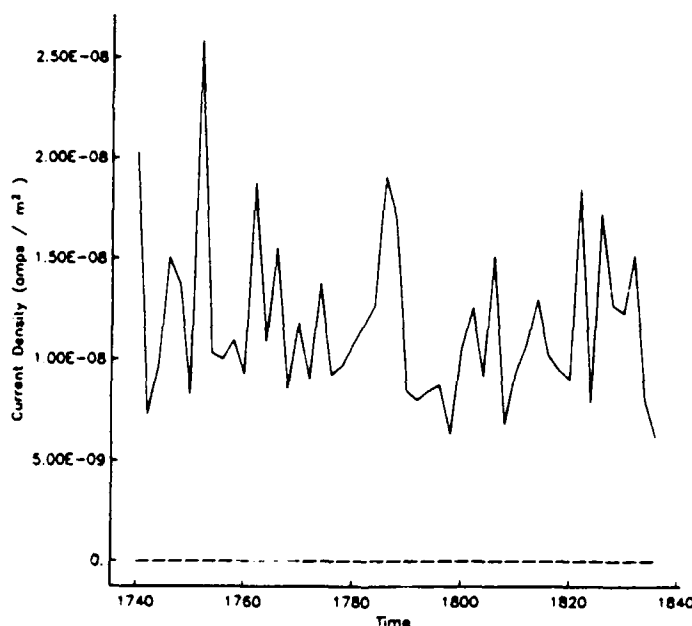

Fig. 4.2 The net electron current density for the period 1,740 to 1,836 of a uniform surface covering of teflon.

coverings, $J_{net}^{electron}$ is always positive for the period 1,740 to 1,836, indicating that the satellite did not charge during this period. This is also true for the other time period (44,100 to 44,160) for teflon but not for kapton. As can be seen in Fig. 4.5, $J_{net}^{electron}$ is negative from 44,114 to 44,124. For these events we can compute a charging potential.
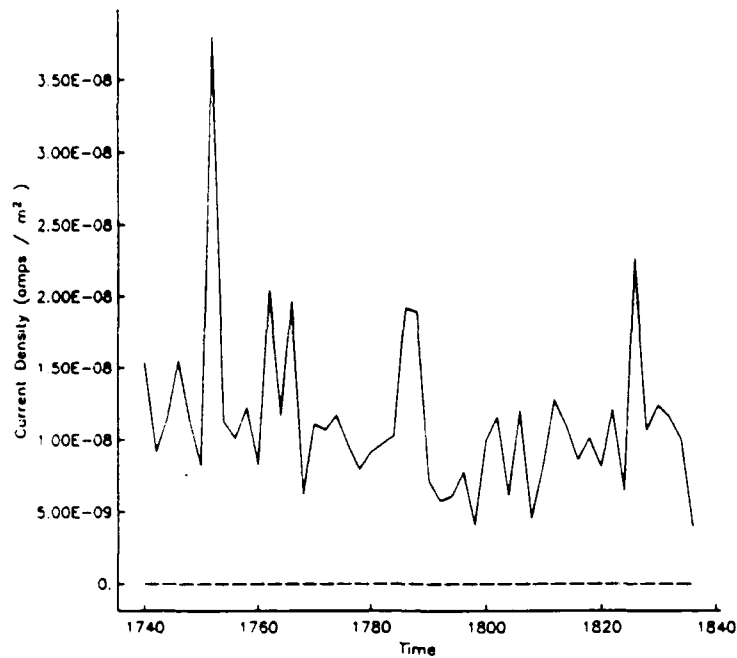
Fig. 4.3 The net electron current density for the period 1,740 to 1,836 of a uniform surface covering of kapton.
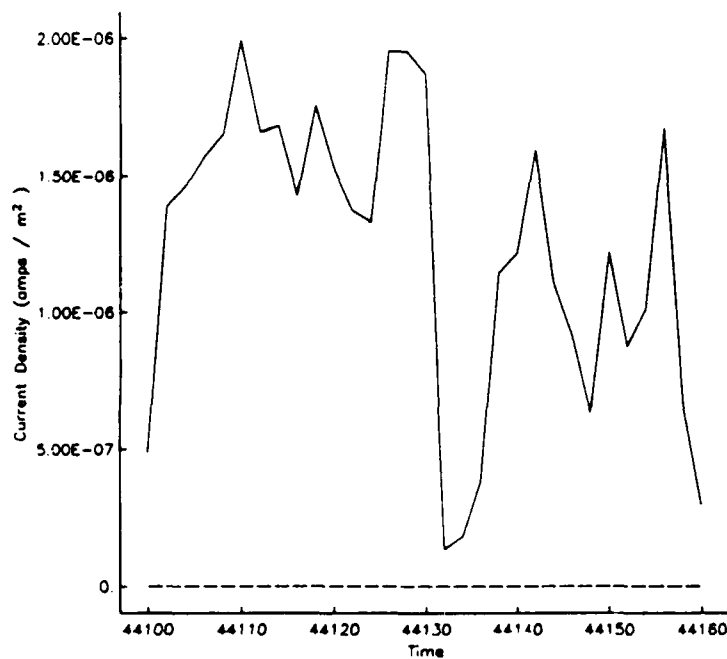

Fig. 4.4 The net electron current density for the period 44,100 to 44,160 of a uniform surface covering of teflon.
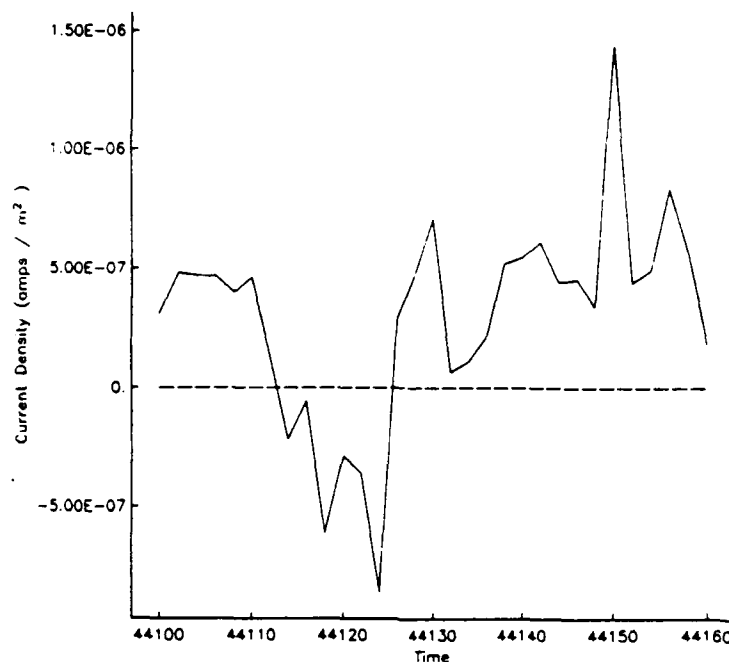
Fig. 4.5   The net electron current density for the period 44,100 to 44,160 of a uniform surface covering of kapton.

Assuming that ion collection is orbit-limited, we may use (4.1) and (4.2) to find the potential. These equations require the ion density n_{ion}, which is sometimes known from independent measurements on the satellite but was not available for these data sets. We have calculated the voltage for three values of n_{ion} with a low, high, and mean value. The results are given in Table 4.1.

Table 4.1   Charging potentials (volts) for three values of ion density

Ion Density $(1/m^3)$

Time	10^6	10^7	10^8
44,114	284.1	23.9	2.1
44,116	65.5	2.0	4.3
44,118	794.2	74.9	3.0
44,120	355.5	31.0	1.4
44,122	466.9	42.2	0.3
44,124	1,209.8	116.5	7.1

Note: No charging is found for ion densities $> = 10^9 /m^3$
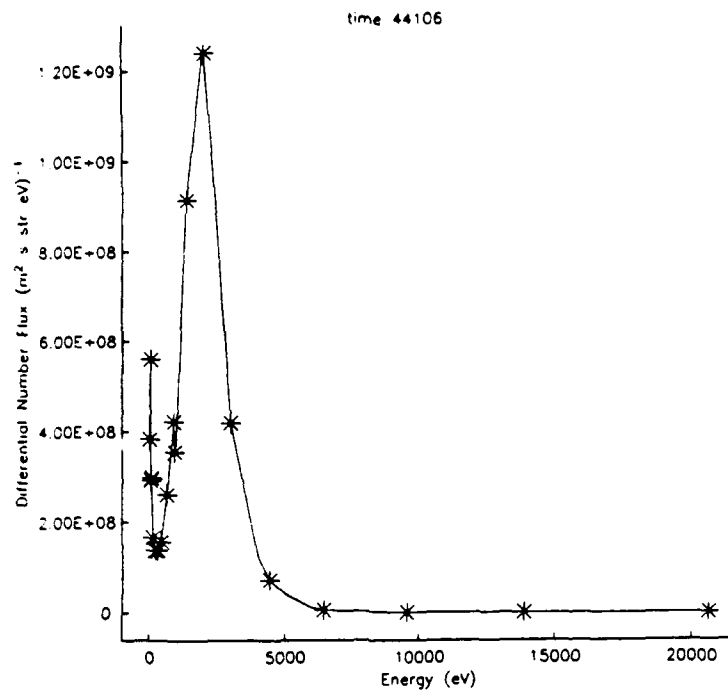
time 44106

Fig. 4.6   The observed differential flux spectrum at time 44,106, a noncharging event, is shown.   Asterisks (*) indicate data values.
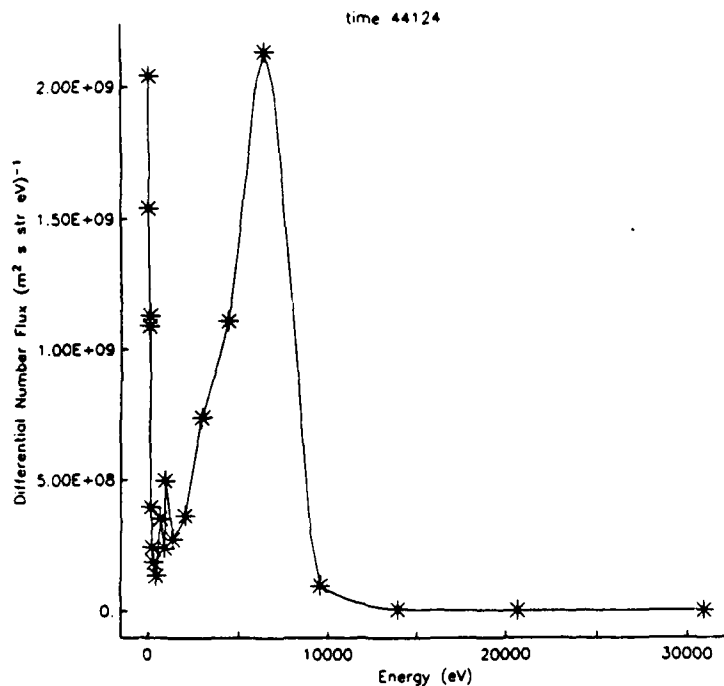
time 44124

Fig. 4.7   The observed differential flux spectrum at time 44,124, a charging event, is shown.   Asterisks (*) indicate data values.

In Fig. 4.6 and 4.7, we show two electron spectra. The first, at time 44,106, is before the charging episode identified above; and the second, at time 44,124, is during the episode. The spectra are similar in that both have peaks in the high energy part of the spectrum. However, the peak in the charging spectrum is at 6.5 keV, while the noncharging spectrum is at 2 keV. Table 4.2, which lists the amplitudes of peaks and the energies at which they occur for times before, during, and after the episode, show that the peaks are consistently above 2 keV for the charging events and below this level for noncharging events. The correspondence between charging and the amplitude of the peaks is not clear, as seen in the table.

Table 4.2   Energies and amplitudes of peaks in electron spectra

Time	Energy (keV)	Amplitude $1.e9/(m^2 \ s \ str \ eV)$	Charge ?
44,106	2	1.2	no
44,108	2	1.3	no
44,110	2	1.8	no
44,112	3	1.4	yes
44,114	4.4	2.6	yes
44,116	4.4	1.9	yes
44,118	4.4	2.4	yes
44,120	4.4	2.1	yes
44,122	4.4	1.5	yes
44,124	6.5	2.1	yes
44,126	2	. 1.3	no
44,128	1.4	2.4	no
44,130	1.4	1.4	no

Katz, Mandell, Jongeward, and Gussenhoven (1986) suggest that large values of the quantities E_{upper} and $E_{charging}$ are correlated with charging. They and Lai et al. (1983) define E_{upper} as the energy below which there is no net current, or

$$\int_{o}^{E_{upper}} [1 - Y(E) - B(E)] \phi_{e|}(E) dE = 0 \tag{4.4}$$

The quantity $E_{charging}$ is the average energy of charging electrons:

$$E_{charging} = \frac{\int_{E_{upper}}^{\infty} [1 - Y(E) - B(E)] E \phi_{e|}(E) dE}{\int_{E_{upper}}^{\infty} [1 - Y(E) - B(E)] \phi_{e|}(E) dE} \tag{4.5}$$

For the spectra in the charging episode, using the kapton yield curves, the values of E_{upper} are 6 - 7 keV and $E_{charging}$ are 7 - 8 keV. These values are about the same as the energy of the peak in the inverted V spectra for the highest charging event.

The next step is to compare the voltages computed and listed in Table 4.1 with other measurements made at the time to see whether they agree, especially if ion density data become available. The correct potentials for the period 44,100 to 44,160 probably lie somewhere between our results for teflon and kapton. This should be resolved and the method should be tested on a more extensive data set.

REFERENCES

Barker, T. G.; "Analytic and Observational Approaches to Spacecraft Auroral Charging"; Report AFGL-TR-87-0021, ADA181456, S-CUBED Report R-87-8377, Air Force Geophysics Laboratory, Hanscom Air Force Base, Massachusetts, 1986.

Hardy, D. A., W. J. Burke, and M. S. Gussenhoven; "Average Worst-Case Specifications of Precipitating Auroral Electron Environment"; paper presented at Spacecraft Environment Interaction Technology Conference, Air Force Academy, Colorado Springs, Colorado, 1983.

Hardy, D. A., and M. S. Gussenhoven; "A Statistical Study of Auroral Electron Precipitations"; J. Geophys. Res., 90 (A5), 4229-4248; 1985.

Hardy, D. A., L. K. Schmitt, M. S. Gussenhoven, F. J. Marshall, H. C. Yeh, T. L. Schumaker, A. Huber, and J. Pantzis; "Precipitating Electron and Ion Detectors (SSJ/4) for the Block 5D/Flights 6-10 Satellites: Calibration and Data Presentation"; Report AFGL-TR-84-0317, ADA157080, Air Force Geophysics Laboratory, Hanscom Air Force Base, Massachusetts, 1984.

Katz, I., J. J. Cassidy, M. J. Mandell, G. W. Schnuelle, P. G. Steen; "The Capabilities of the NASA Charging Analyzer Program"; paper presented at Spacecraft Environment Interaction Technology Conference, Air Force Academy, Colorado Springs, Colorado, 1978.

Katz, I., M. Mandell, G. Jongeward, and M. S. Gussenhoven; "The Importance of Accurate Secondary Electron Yields in Modeling Spacecraft Charging"; J. Geophy. Res., 91 (A12), 13,739-13,744, 1986.

Katz, I., D. E. Parks, M. J. Mandell, J. M. Harvey, D. H. Brownell, S. Wang, M. Rotenberg; "A Three Dimensional Dynamic Study of Electrostatic Charging in Materials"; NASA CR-135256, S-CUBED Report R-77-3367, 1977.

Lai, S. T., M. S. Gussenhoven, and H. A. Cohen; "The Concepts of Critical Temperature and Energy Cutoff of Ambient Electrons in High Voltage Charging of Spacecraft"; Proceedings of the 17th ESLAB Symposium on Spacecraft/Plasma Interactions and Their Influence of Field and Particle Measurements"; Noordwijk, The Netherlands, 1983; ESA SP-198, 169-175, 1983.

Langlet, R. A., J. Bodhansky, W. Ekstein, P. Mioduszewski, J. Roth, E. Taglauer, E. W. Thomas, H. Verbeek, and K. L. Wilson; "Data Compendium for Plasma-Surface Interactions"; Nuclear Fusion Special Issue, 1984.

Lilley, J. R., Jr., D. L. Cooke, G. A. Jongeward, and I. Katz; "POLAR User's Manual"; S-CUBED Report R-86-7563, 1985. AFGL-TR-85-0246 ADA173758

Meng, C. I.; "Electron Precipitations and Polar Auroras"; Space Science Reviews, 22, 223-300, 1978.

Olsen, R. C.; "A Threshold Effect for Spacecraft Charging"; J. Geophys. Res., 88, 493, 1983.

Tanskanen, P. J., D. A. Hardy, and W. J. Burke; "Spectral Characteristics of Precipitating Electrons Associated with Visible Aurora in the Premidnight Oval During Periods of Substorm Activity"; J. Geophys. Res., 86 (A3), 1,379-1,395, 1981.